Nanoscale

REVIEW

Charge transport at the metal oxide and organic interface

Zhenhuan Zhao,[a] Hong Liu*[ab] and Shaowei Chen*[c]

This review focuses on electron transfer at the interfaces between metal oxides and dye molecules within the context of the chemical nature of the anchoring functional groups, the structure of the dye molecules and the morphology of the metal oxides. In dye-sensitized metal oxides, the efficiency of interfacial charge separation and hence photon-to-current conversion may be sensitively manipulated by the interfacial bonding interactions whereby the dye molecules are adsorbed onto the oxide surface, as well as by the oxide surface morphologies. In these studies, it has been found that upon photoirradiation, the electron injection from the excited dye molecules into the conduction band of metal oxides and electron transport in the metal oxide are two of the most important steps. Therefore, a fundamental understanding of how the interfacial electron transfer dynamics is impacted by these structural parameters is critical for the design and optimization of dye-sensitized photocatalysis and photovoltaics.

1   Introduction

In the unremitting pursuit of efficient utilization of solar energy, scientists have devoted great efforts to the development of new functional materials. Among these, metal oxides with a wide band gap have been found to be an important and useful material that may realize the efficient separation and fast transport of photogenerated electrons. Furthermore, the transfer rate and concentration of charge carriers may be enhanced when the metal oxide is sensitized with dye molecules.

In these dye-sensitized oxide systems, there are at least five main electron transfer processes, as shown in Fig. 1.[1] It is important to control the dynamics of photogenerated electrons in each process. According to the Marcus theory, efficient charge separation requires the rate of electron injection (k_{inj}) to be faster than that of the decay from the dye excited state to the ground

[a]State Key Laboratory of Crystal Materials, Center of Bio & Micro/Nano Functional Materials, Shandong University, 27 S. Shanda Road, Jinan 250100, China. E-mail: hongliu@sdu.edu.cn

[b]Beijing Institute of Nanoenergy and Nanosystems, Chinese Academy of Sciences, Beijing, China

[c]Department of Chemistry and Biochemistry, University of California, 1156 High Street, Santa Cruz, California 95064, USA. E-mail: shaowei@ucsc.edu
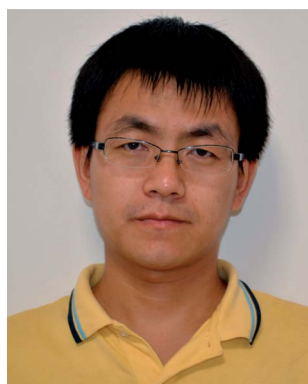
Zhenhuan Zhao obtained his M.Sc. degree from Shandong Polytechnic University, China, in 2011. Currently he is pursuing his Ph.D. under the supervision of Prof. Hong Liu and Prof. Shaowei Chen at the State Key Laboratory of Crystal Materials, Shandong University, China. His research interests are mainly focused on the preparation of surface multi-hetero-structures based on TiO$_2$ nanomaterials for photo-catalysis and energy storage applications.

Zhenhuan Zhao

Hong Liu received his B.Sc degree from Shandong Institute of Light Industry in 1985, and his Ph.D. from Shandong University in 2001. In 2002, he joined the State Key Laboratory of Crystal Materials, Shandong University, China, as a professor. His research is focused on the synthesis of nanomaterials and their applications in gas sensing and bio-sensing, environmental protection, new energy sources, and biomedical applications. He has published more than 100 peer-reviewed research articles and 25 patents.

Hong Liu
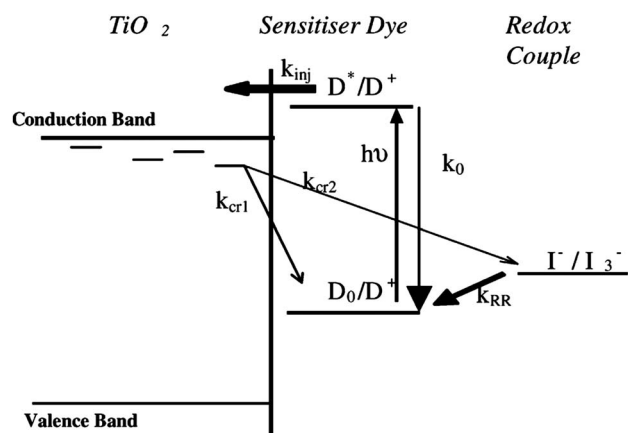
Fig. 1 Schematic diagram showing the different interfacial electron transfer processes: injection from dye excited state into the conduction band of metal oxide semiconductor (k_{inj}); regeneration of the dye cation by electron transfer from the redox couple (k_{RR}); recombination of electron with the dye cation (k_{cr1}); electron recombination to the redox couple (k_{cr2}) and excited state decay to ground (k_0). Reproduced by permission from ref. 1, copyright (2002) Elsevier Science B.V.

state (k_0).[2] Meanwhile, the dye cation re-reduction by the redox couple in the electrolyte solution (k_{RR}) should also be faster than recombination between the injected electrons and photo-produced dye cations (k_{cr1}). Furthermore, charge recombination between the injected electrons and oxidized redox species (k_{cr2}) should be slower than the transport of these charges.[3] Therefore, one can see that charge transfer at the metal oxide interface is influenced by the physicochemical properties of the metal oxide and the dye molecule, in particular, the ground and excited electronic states of the dye molecule. As metal oxide semiconductors with different morphologies and wide band gaps are usually used as substrates for dye sensitization,[4–7] the review will highlight some of the recent progress in these areas.

In this review article, we will summarize research in the chemical modification of metal oxides by dye molecules with

Shaowei Chen

Shaowei Chen finished his undergraduate studies in China in 1991 with a B.Sc. degree in Chemistry from the University of Science and Technology of China, and then went to Cornell University receiving his M.Sc. and Ph.D. degrees in 1993 and 1996, respectively. Following a postdoctoral appointment at the University of North Carolina at Chapel Hill, he started his independent career in Southern Illinois University in 1998. In 2004, he moved to the University of California at Santa Cruz and
is currently a Professor of Chemistry. His research interests are primarily in the electron transfer chemistry of nanoparticle materials.

different anchoring groups which chemically link the ligands to the metal oxide surfaces and examine their impacts on the interfacial electron transfer dynamics. The effects of the surface morphologies of metal oxides will also be discussed.

2 Effects of anchoring groups

Interfacial electron transfer between adsorbed dye molecules and metal oxide substrates is considered to be the key process of dye-sensitized metal oxide systems in photoelectrochemistry,[8] solar energy conversion,[9–11] and artificial photosynthesis.[12] The dye molecules can be physically adsorbed onto the metal oxide surface, or form covalent bonds. Compared to physisorption, the formation of covalent bonds not only increases the stability and even distribution of the dyes on the metal oxide surfaces, but also increases the strength of the electronic coupling and thus may lead to enhanced electron injection.[13] There are a variety of functional moieties that have been used to bridge dye molecules to metal oxides, including carboxylate,[14–17] phosphonate,[18–22] siloxane,[23,24] acetylacetonate,[25–27] salicylate,[28] catechol,[29–31] and so on. The attachments of chromophoric or non-chromophoric ligands onto the surface of oxide semiconductors by these anchoring moieties offer various unique advantages such as the extended absorption of visible light, long lifetimes of the excited states, stable oxidized and reduced forms, *etc.*, which are critical for the enhancement of the efficiency of photoenergy conversion.

2.1 Carboxyl groups

In dye-sensitized photocatalysis and photovoltaics, dye molecules grafted on the surface of metal oxides are excited and subsequently inject electrons into the conduction band of metal oxides to generate a photocurrent by interfacial electron transfer (Fig. 1). The fate of the injected electrons significantly depends on the process of interfacial electron transfer under photo-irradiation, which may be varied by the surface states and crystallinity of the metal oxides. In addition, the dye molecules also play an important role. For ideal dyes, they are expected not only to maximize the utilization of the solar energy, but also to form stable interfacial electronic couplings with metal oxides and hence facilitate interfacial charge transfer.

One of the most popular anchoring groups for ruthenium sensitizers is carboxylate. Carboxylate forms bonds with surface hydroxyl groups and the binding is reversible with a high equilibrium constant.[32] The linking between the dye molecule and metal oxide includes various forms, such as ester bonds with monocarboxyl groups anchored onto the titanium sites, or carboxylato linkages with two carboxyl groups anchored onto two titanium sites (Fig. 2).[33] In the latter form, the oxygen atoms may be from the same or neighbouring bipyridine ligands. Infrared and Raman spectroscopic analyses of Ru(II) dyes, as well as the corresponding dye-sensitized TiO$_2$ photoelectrodes, indicate that the carboxylates graft to the TiO$_2$ surface *via* bidentate chelation or bridging coordination with two carboxylate groups per dye molecule.[34] Further research shows that the dyes bond to the surface of TiO$_2$ in a bridging mode with both oxygen atoms from an anchoring carboxyl group interacting with adjacent titanium atoms, though not all carboxyl groups participate in binding to

Fig. 2 Structures of the possible surface complexes of (a) carboxyl–RuL₃ and (b) phosphonate–RuL₃. Reproduced by permission from ref. 33, copyright (2004) American Chemical Society.

titanium atoms.[35] After modification by dye molecules, the metal oxides usually display a change in their electronic properties. For instance, the fluorescence characteristics of 9-anthracene-carboxylic acid-modified TiO_2 particles are very different from those of the free dyes in solution.[14] The adsorbed dye molecules exhibit a structured spectrum with a small Stokes shift, while the free molecules display a broad and red-shifted spectrum. The red shift is ascribed to the stabilization of the excited electronic state through torsional motion of the carboxylate group. The grafting of carboxyl groups to TiO_2 has been shown to serve as the interlocking agent coupling electronically the π* orbitals of the ligand to the Ti 3d orbitals. The strongly covalent ester linkage is greatly beneficial to the electron transfer injection during the photoelectrochemical processes.[36]

The number and position of carboxyl groups grafted to ligands have also been found to impact the interfacial electron transfer dynamics. Hara et al.[37] have reported that the absorbed photon-to-current conversion efficiency was lower with monocarboxyl groups grafted to TiO_2 than that of complexes with two or more carboxyl groups grafted to TiO_2. This is largely because the interfacial electronic coupling with two anchoring carboxyl groups is larger than that with only one carboxyl group. Additionally, electronic coupling is usually sensitive to the relative configuration between the excited dye molecule and the metal oxide surface. They concluded that for an effective electron injection into the conduction band of TiO_2, two carboxyl groups as the anchors were necessary. Tachibana et al. modified the surface of TiO_2 by using the ruthenium dye, $Ru^{II}(2,2'$-bipyridy-4,4'-dicarboxylate)$_2(NCS)_2$, which has four carboxyl groups, and observed ultrafast electron injection kinetics.[38] Nonetheless, it should be pointed out that dyes with only one carboxyl group as the anchoring group have also been used as sensitizers and displayed an efficiency of electron injection that is comparable with that possessing more than one carboxyl group.[6,39,40] In general, the number of carboxyl groups available to form a favourable anchoring geometry for the effective injection of electrons depends upon the molecular structure of the ligands linked to the carboxyl group.

In addition, some prior reports have shown that the carboxyl groups attached to the meso-phenyl ring of the porphyrin molecule exert little influence on the ground state of the dye molecule. This is ascribed to the low energy conformation of the phenyl groups which are arranged in an idealized orthogonal orientation with regard to the mean plane of the porphyrin moiety.[41] However, much work has shown that the position of the carboxyl group may significantly affect the properties related to interfacial electron transfer. For example, although dye-sensitized TiO_2 with both 4,4'–(COOH)₂–2,2'-bipyridine $Ru(NCS)_2$ and 5,5'–(COOH)₂–bipyridine 2,2'-Ru(NCS)₂ displays ultrafast (<350 fs) electron injection, the electron injection from the latter dye apparently exhibits a lower quantum yield than that from the former one.[15] Odobel et al. have demonstrated that dyes with the carboxyl group anchoring directly onto the π-aromatic core of the porphyrin ligand gave rise to stronger electronic interactions with TiO_2 than dyes with the carboxyl group far away from the porphyrin macrocycle.[42]

With the anchoring of carboxyl groups to the surface of metal oxides, the surface states of metal oxides can be altered significantly. It should be noted that whereas the number and position of carboxyl groups impact electron transfer at the interface between dye molecules and metal oxides, the chemical bridge which links the carboxyl group and the excited center may also exert an influence on the electron transfer that limits and promotes light energy conversion. The bridge varies the distance between the anchoring group and the excited center to the ligand. Hara and co-workers[40] have reported that the introduction of a –CH=CH– unit into the coumarin framework (C343 in Fig. 3) may shift the threshold wavelength of absorption from 500 to 570 nm for molecule **1** and to 600 nm for molecule **2**. The red-shift of the threshold wavelength may improve the efficiency of light harvesting of solar energy. The reason is that the
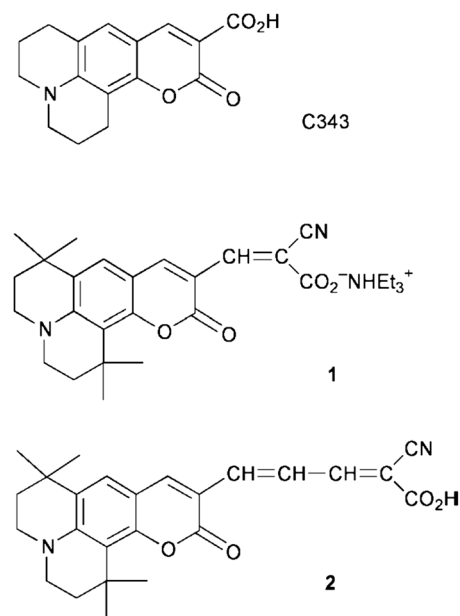
Fig. 3 Molecular structure of coumarin derivatives. Reproduced by permission from ref. 40, copyright (2001), the Royal Society of Chemistry.

introduction of –CH=CH– extends the conjugation in the dye molecules leading to wide adsorption in the visible region.[40] If –CH=CH– is substituted by a xylyl group, the interfacial kinetics of Ru(II) complex-sensitized nanocrystalline TiO$_2$ are consequently changed. It is found that the rate constant for electron injection decreases by no more than a factor of 2 as the Ru-to-COOH distance increases from 13.8 to 22.5 Å, and the rate constant for the recombination of injected electrons with the oxidized dye increases slightly with increasing linker length. Both the quantum yield for the conversion of absorbed photons to current and the magnitude of the open-circuit voltage decrease with increasing linker length (Fig. 4).[43] A possible explanation is that the single carboxyl anchoring group makes the connection to TiO$_2$ flexible resulting in a decrease of the Ru–TiO$_2$ electron tunnelling distance. Methylene groups can also be used to adjust the electron transfer rate. With more than eight methylene units, the electron transfer rate constant is found to vary exponentially with the number of methylene units.[44,45] In the case of only one or two methylene units, the dyes with anchoring carboxyl groups display a non-exponential correlation of electron injection. In the case of three to five CH$_2$ groups, the electron injection constant rate decreases exponentially with the number of methylene units (Fig. 5).[46]

2.2 Phosphonate

As mentioned above, carboxylate dyes may covalently graft onto the metal oxide surface, act as a charge transfer sensitizer injecting electrons from the metal centre into the conduction band of the semiconductor, and display a high incident photon-to-current conversion efficiency. Nonetheless, carboxylic-based chemical bonding is typically susceptible to hydrolysis. Stronger and more stable linkages are thus desired, which may be formed with phosphonate derivatives,[22,33,47,48] especially in organic solvents.[21,49–51]

Notably, phosphonate linkages are generally more stable in a wider pH range than carboxylic linkages.[33] It has been reported that dyes containing carboxyl groups desorb whereas phospho-nated dyes remain intact when they sensitize TiO$_2$ in water at pH values of 5–6. Further investigations have shown that the discrepancy may arise from the differences in the dissociation constants of the ligands.[20] It is well-known that electron transfer rates depend on the density of accepting states in the semiconductor due to the existence of a quasi-continuum of electronic states. It is also known that the density varies with the position of the excited state oxidation potential of the adsorbed dye relative to the conduction band of the semiconductor. Since the
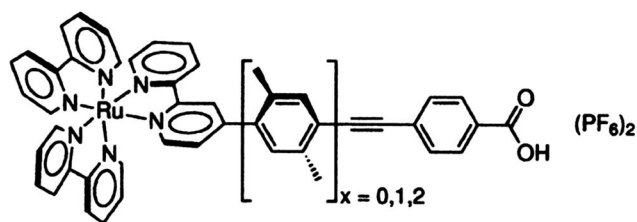
Fig. 4 Molecular structure of Ru(II) dyes with varied xylyl spacers. Reproduced by permission from ref. 44, copyright (2003), the American Chemical Society.
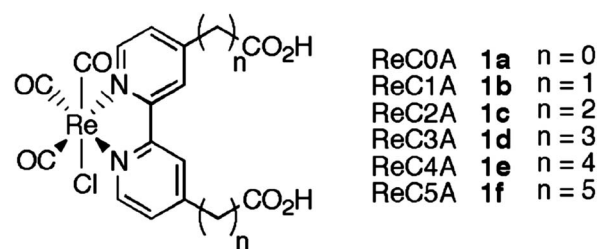
Fig. 5 Dyes with n = 1 to 5 methylene bridging groups between the bipyridine and the carboxyl group. Reproduced by permission from ref. 46, copyright (2003), the American Chemical Society.

conduction band edge position changes with the pH of the solution, the interfacial electron transfer rates show pH dependence.

The length of the chemical spacer between the phosphonate moiety and the chromophoric ligand also has an effect on the photocurrent efficiency. It is reported that by introducing a methylene spacer between the phosphonate group and the bipyridine ligand the photocurrent efficiency and the electron injection quantum yield decrease significantly.[51]

2.3 Siloxane and other groups

Extensive research has also been carried out for the discovery of new anchoring groups to enhance the electron injection from chromophores to semiconductor surfaces, to decrease the back electron transfer dynamics and finally to obtain a high photon-to-current conversion efficiency. In addition to carboxyl and phosphonate groups, many more moieties have been used to bridge the chromophoric ligands to the semiconductors, such as siloxane, acetylacetonate, and catechol.

Siloxane is an effective anchoring group to bridge ligands to metal oxide surfaces by way of covalent bonding.[52] Siloxane-functionalized semiconductors have been found to show fast electron injection from the metal centre to the conduction band of the semiconductor, with the recombination process hindered between the oxidized metal centre and the injected electrons in the semiconductor, leading to a high photon-to-current conversion efficiency.[23] In the attachment of siloxane adsorbates on TiO$_2$ surfaces, it has been demonstrated that the bridge binding is more stable than tripod geometry, i.e., two siloxane groups form covalent bonds with adjacent Ti^{4+} on the surface of TiO$_2$.[24,53]

In some other studies, acetylacetonate derivatives have been found to form adducts with Ti^{3+} compounds, which are stable towards hydrolysis reactions over a wide pH range, allowing for potential applications in optoelectronic fields.[27] Acetylacetonate exhibits less intimate electronic coupling between the oxide surface and the chromophoric ligand than the carboxyl group. However, sensitizers with the acetylacetonate group still exhibit a photon-to-current conversion efficiency comparable to that of carboxyl groups.[25] Another advantage of using acetylacetonate derivatives as the anchoring group is that they can attach a broad range of photosensitizers, and the photocatalytic complexes are not affected by humidity, such as transition metal–pyridine complexes. For example, TiO$_2$ sensitized by Mn(II) terpyridine complexes with acetylacetonate as the anchoring moiety show that an interfacial electron transfer process can be achieved

under visible light illumination, and the rate constant of interfacial electron transfer is on the sub-picosecond time scale.[26]

Anchoring by catechol may also extend the light adsorption of metal oxides to the visible region. It has been found that the recombination between the electrons injected into TiO_2 nanoparticles and the oxidized adsorbates is much faster than that in dye-sensitized thin films.[29,54] The catechol moiety forms a five-membered ring with Ti^{4+} on the surface of TiO_2 nanoparticles, giving rise to the formation of the charge transfer complex.[30,31,55]

3 Effects of oxide morphology

Interfacial electron transfer in nanosized materials also varies with the size and morphology of the nanomaterials. When a bulk material is reduced in size to the nanoscale, the specific surface area and number of surface atoms will increase dramatically with respect to the size, and their chemical activities and optical properties change significantly. A variety of nanomaterials have been used in solar cell applications, including nanoparticles,[56–58] nanorods,[59,60] nanotubes,[61] nanowires,[62,63] nanobelts,[64–66] nanoplates,[67–69] etc.

3.1 Nanoparticles

The photon-to-current conversion efficiency of dye-sensitized solar cells is determined by the population and lifetime of the charge carriers and the time scale of the interfacial electron transfer process. To date, rather thorough investigations have been carried out and a good understanding has been obtained of the mechanism and electron transfer involved in practical applications. Nanoparticles with high specific surface areas are one of the most promising dye-sensitized systems for solar light harvesting and conversion. When nanoparticles are used as electrode materials, the large specific surface area relative to the particle size greatly influences the effective surface area of the photoelectrodes. Taking ZnO as an example, it has been found that the overall solar energy conversion efficiency is as high as 2% for ZnO films consisting of 15 nm crystallites, while only 0.5% for films with 150 nm large crystallites.[70] The size of the particles also shows an influence on the binding forms of the anchoring groups on the surface of metal oxides. For example, the binding of the carboxylic anchoring group on the surface of TiO_2 evolves from physical adsorption and hydrogen bonding to chemical binding when the size of the TiO_2 nanoparticles decreases from 6 nm to less than 1.4 nm.[17]

3.2 Nanorods

One dimensional nanostructures have also been used as excellent electrode materials for dye-sensitized solar cells due to the unique physical and chemical properties.[71,72] Nanorods have been widely used as photoelectrode materials for the ready transport of injected electrons along the vertical direction.[73] One-dimensional materials usually have a lower trap density and more direct paths as the current-collecting electrode than (spherical) colloidal counterparts, and thus they are expected to facilitate charge transfer. For example, the electron transfer in solar cells with ZnO nanorods is about two orders of magnitude faster than that with ZnO colloidal nanoparticles (Fig. 6).[74] Strategies used to further improve the photon-to-current conversion efficiency
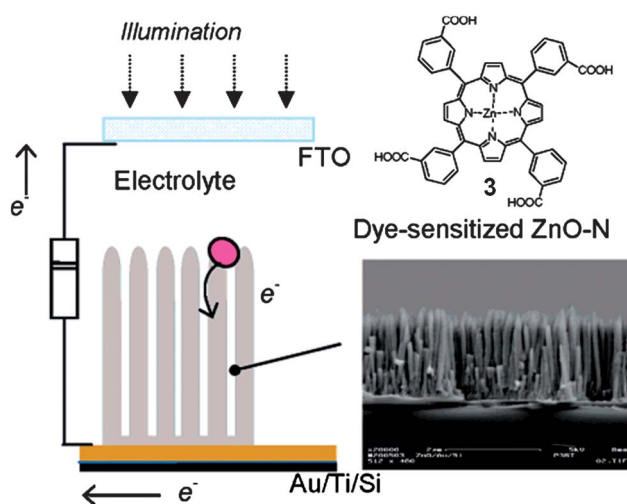
Fig. 6 Schematic representation of the ZnO-nanorod cell sensitized with **3**. The gold layer is deposited on a silicon substrate. Reproduced by permission from ref. 74, copyright (2006), the American Chemical Society.

involve lengthening the nanorods and enlarging the space between the nanorods in the array for efficient utilization of incident light, improving the crystallinity to eliminate the effects of grain boundaries, and lowering the number of defects that may be barriers to electron transfer.

Note that the crystallinity of nanorods greatly depends on the preparation methods. Gao et al. have investigated the effects of the preparation methods on the performance of the corresponding dye-sensitized solar cells.[75] The results show that ZnO nanorods prepared from multi-step hydrothermal growth for a total of 48 h exhibit higher crystallinity and a lower level of defects than those obtained from one-step hydrothermal growth for 10 h, and solar cells with the former display a faster electron transfer and higher efficiency than with the latter. Tornow and Schwarzburg have also demonstrated the importance of the crystallinity of nanorods.[76] Solar cells with single crystalline anatase TiO_2 nanorods prepared from a hydrothermal process
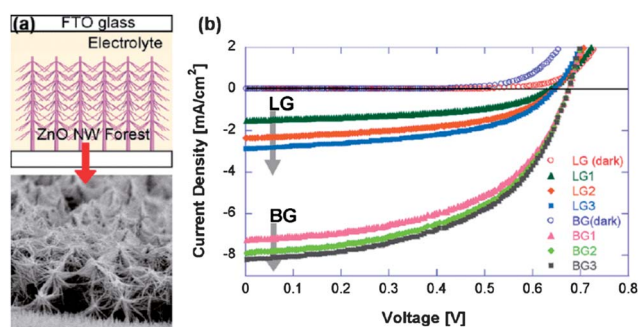
Fig. 7 (a) Schematic structure and (b) J–V curves of dye-sensitized solar cells with nano-forest ZnO nanowires of various lengths. LG and BG refer to samples from the length and branched growth, respectively. LG1: 7 μm, LG2: 13 μm, LG3: 16 μm. BG1 and BG2 refer to the one-time branched growth on LG1 and LG2, respectively; BG3 refers to the two-time branched growth on LG3. Reproduced by permission from ref. 87, copyright (2011), the American Chemical Society.
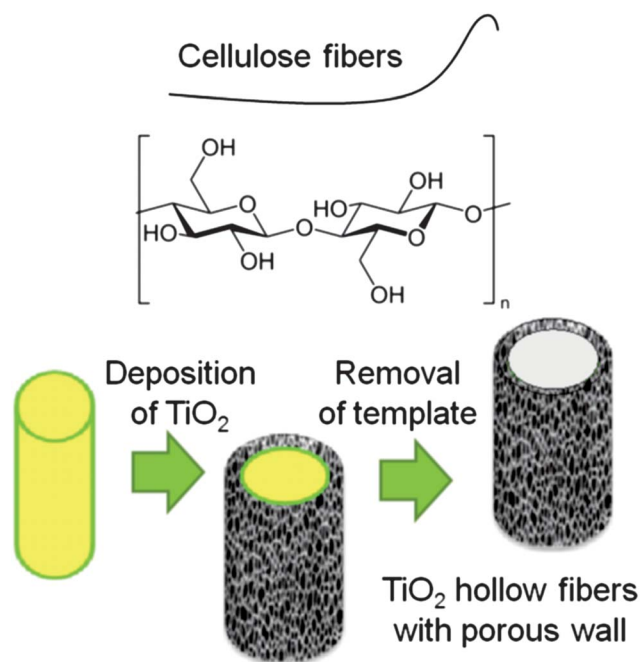
Fig. 8 Scheme of TiO$_2$ hollow fibre preparation steps. Reproduced by permission from ref. 88, copyright (2010), the American Chemical Society.

display a high photon-to-current conversion efficiency of 7.29%.[77]

To further improve the efficiency of solar cells, Lee et al. prepared TiO$_2$ nanorods by the electrospinning method and used them for solar cell applications. They found that TiO$_2$ nanorods have a higher sensitizing capability and much lower recombination lifetimes than nanoparticles. When the nanorods were post-treated with TiCl$_4$, the electron transport behaviours of the nanorod photoelectrodes were improved, and the electron diffusion coefficient was greater than that of the untreated one.[78] When ZnO nanorods were decorated with gold nanoparticles, the adsorption of light was extended into the visible region because of the plasmonic absorption properties of gold nanoparticles. At the same time, the Schottky barrier between the gold nanoparticles and ZnO nanorods blocks the back transfer of electrons from ZnO to the dye molecule and electrolyte, leading to the increase of electron density. Furthermore, when gold-decorated ZnO nanorods were sensitized with dyes, the open circuit voltage increased significantly, compared to that of bare ZnO nanorods.[79] Another method is to use oxide nanorods as the basic materials to form hybrid structures with conductive polymers.[80–83]

3.3 Nanotubes and nanowires

Nanotubes possess not only the advantages of nanorods, but also other unique characteristics, such as large specific surface areas and open structures. It has been shown that the performance of TiO$_2$-based dye-sensitized solar cells may be closely related to the high surface area of the titania electrode films. The large surface area can endow the electrode with a high adsorption coefficient for dye molecules as well as easy penetration of the polymer

electrolyte.[84] Martinson et al. have reported a solar cell with ZnO nanotubes prepared by using anodic aluminum oxide as the template. Under AM 1.5 illumination, the most efficient cell showed a short-circuit photocurrent density of 3.3 mA cm^{-2} and open-circuit photovoltage of 739 mV, leading to an overall conversion efficiency of 1.6%.[61] The highly ordered nanostructures allow for improved charge separation and charge transport. Mor et al. have prepared a solar cell based on TiO$_2$ nanotube arrays with a short-circuit photocurrent of 7.87 mA cm^{-2} and an open-circuit photovoltage of 750 mV, leading to a photoconversion efficiency as high as 2.9%.[85] Increasing the length of the nanotubes may also improve the solar cell efficiency. Liu and Misra have prepared ultralong TiO$_2$ nanotubes with a length of 55 μm and obtained a photo-to-current conversion efficiency of 2.78% under 1.5 AM simulated light illumination. The ultralong nanotubes can harvest light from any direction.[86]

Among the one-dimensional materials, nanowires have also been recognized as promising candidates for solar cell applications. Nanowires with a good control of crystallinity provide a direct path for electron transfer, and thus a high solar cell efficiency can be achieved. Feng et al. have reported a hydrothermal method to prepare single crystalline TiO$_2$ nanowires on the ITO surface. Solar cells based on dye-sensitized TiO$_2$ nanowires reach a photoconversion efficiency of 5.08% under 1.5 AM light illumination. The efficiency is thought to be attributed to the length and crystallinity of the nanowires.[63] However, the large number of oxygen vacancies in TiO$_2$-B nanowires may act as recombination centres or trapping states of the charge carriers, thus compromising the photocurrent efficiency.[62] An effective method to improve the solar cell efficiency with ZnO nanowires is to prepare branched ZnO nanowires. Very recently, Ko et al. have reported tree-like hierarchical ZnO nanowires whose overall light conversion efficiency is almost 5 times higher than that of unstanding ZnO nanowires. This is ascribed to the enhancement of surface area for high dye-loading and efficient light harvesting, as well as to the diminishment of charge recombination (Fig. 7).[87] By using natural cellulose fibres as a template, hollow TiO$_2$ nanofibres have also been prepared for solar cell utilization, and the electron transport and photoinjected electron lifetime are remarkably enhanced (Fig. 8).[88]

4   Conclusion

The performance of dye-sensitized photoelectrochemical systems is dependent upon several critical structural parameters. Among these, the efficiency of the separation of photogenerated electrons may be sensitively varied by the interfacial interactions between the dye molecules and the oxide substrates. For enhanced photon-to-current conversion, covalent bonding rather than simply physisorption is preferred for the grafting of organic dye ligands to the metal oxide surfaces. Covalent bonding enhances the electronic coupling which is beneficial to electron injection from the dye excited state into the conduction band of the metal oxide. The structures of the dye molecules also exert effects on the electron transfer dynamics at the interface between the dye and the metal oxide, in particular, with regards to the lifetime of the excited state of the dye molecules. Furthermore, the surface morphologies of the metal oxides also display significant impacts

on the oxide electronic properties, and one-dimensional metal oxide nanostructures have been found to provide a direct access for electron transport, where the electron transfer rate in the metal oxide can be enhanced by improving the oxide crystallinity. Notably, although substantial progress has been made in these research areas, it is of critical importance to further advance our understanding of the fundamental mechanisms behind these interfacial processes, such that rational designs and the optimization of next-generation dye-sensitized metal oxide photoelectrochemical systems can be achieved.

Acknowledgements

References

1 J. R. Durrant, *J. Photochem. Photobiol., A*, 2002, **148**, 5–10.
2 D. M. Adams, L. Brus, C. E. D. Chidsey, C. C. Stephen Creager, C. R. Kagan, P. V. Kamat, M. Lieberman, S. Lindsay, R. A. Marcus, R. M. Metzger, M. E. Michel-Beyerle, J. R. Miller, M. D. Newton, D. R. Rolison, O. Sankey, K. S. Schanze, J. Yardley and X. Zhu, *J. Phys. Chem. B*, 2003, **107**, 6668–6697.
3 J. R. Durrant, S. A. Haque and E. Palomares, *Coord. Chem. Rev.*, 2004, **248**, 1247–1257.
4 R. W. Fessenden and P. V. Kamat, *J. Phys. Chem.*, 1995, **99**, 12902–129066.
5 C. Nasr, S. Hotchandani and P. V. Kamat, *J. Phys. Chem. B*, 1998, **102**, 4944–4951.
6 K. Hara, T. Horiguchi, T. Kinoshita, K. Sayama, H. Sugihara and H. Arakawa, *Sol. Energy Mater. Sol. Cells*, 2000, **64**, 115–134.
7 C. Bauer, G. Boschloo, E. Mukhtar and A. Hagfeldt, *J. Phys. Chem. B*, 2001, **105**, 5585–5588.
8 A. Fujishima, *Nature*, 1972, **238**, 37–38.
9 B. O'Regan and G. Michael, *Nature*, 1991, **353**, 737–740.
10 M. Grätzel, *Nature*, 2001, **414**, 338–344.
11 M. Gratzel, *Philos. Trans. R. Soc. London, Ser. A*, 2007, **365**, 993–1005.
12 M. R. Wasielewski, *Chem. Rev.*, 1992, **92**, 435–461.
13 K. Kalyanasundaram and M. Grätzel, *Coord. Chem. Rev.*, 1998, **77**, 347–414.
14 I. Martini, J. Hodak, G. V. Hartland and P. V. Kamat, *J. Chem. Phys.*, 1997, **107**, 8064–8072.
15 T. A. Heimer, E. J. Heilweil, C. A. Bignozzi and G. J. Meyer, *J. Phys. Chem. A*, 2000, **104**, 4256–4262.
16 M. K. Nazeeruddin, P. Péchy, T. Renouard, S. M. Zakeeruddin, R. Humphry-Baker, P. Comte, P. Liska, L. Cevey, E. Costa, V. Shklover, L. Spiccia, G. B. Deacon, C. A. Bignozzi and M. Grätzel, *J. Am. Chem. Soc.*, 2001, **123**, 1613–1624.
17 Q.-L. Zhang, L.-C. Du, Y.-X. Weng, L. Wang, H.-Y. Chen and J.-Q. Li, *J. Phys. Chem. B*, 2004, **108**, 15077–15083.
18 P. Péchy, F. P. Rotzinger, M. K. Nazeeruddin, O. Kohle, S. M. Zakeeruddin, R. Humphry-Baker and M. Grätzel, *J. Chem. Soc., Chem. Commun.*, 1995, **1**, 65–66.
19 G. B. Saupe, T. E. Mallouk, W. Kim and R. H. Schmehl, *J. Phys. Chem. B*, 1997, **101**, 2508–2513.
20 P. Bonhôte, E. Gogniat, S. Tingry, C. Barbé, N. Vlachopoulos, F. Lenzmann, P. Comte and M. Grätzel, *J. Phys. Chem. B*, 1998, **102**, 1498–1507.
21 S. A. Trammell, J. A. Moss, J. C. Yang, B. M. Nakhle, C. A. Slate, F. Odobel, M. Sykora, B. W. Erickson and T. J. Meyer, *Inorg. Chem.*, 1999, **38**, 3665–3669.
22 S. G. Yan, J. S. Prieskorn, Y. Kim and J. T. Hupp, *J. Phys. Chem. B*, 2000, **104**, 10871–10877.
23 W. E. Ford and M. A. J. Rodgers, *J. Phys. Chem.*, 1994, **98**, 3822–3831.
24 F. Milanesi, G. Cappelletti, R. Annunziata, C. L. Bianchi, D. Meroni and S. Ardizzone, *J. Phys. Chem. C*, 2010, **114**, 8287–8293.
25 T. A. Heimer, S. T. D'Arcangelis, F. Farzad, J. M. Stipkala and G. J. Meyer, *Inorg. Chem.*, 1996, **35**, 5319–5324.
26 W. R. McNamara, R. C. Snoeberger III, G. Li, J. M. Schleicher, C. W. Cady, M. Poyatos, C. A. Schmuttenmaer, R. H. Crabtree, G. W. Brudvig and V. S. Batista, *J. Am. Chem. Soc.*, 2008, **130**, 14329–14338.
27 T. T. O. Nguyen, L. M. Peter and H. Wang, *J. Phys. Chem. C*, 2009, **113**, 8532–8536.
28 J. Moser, S. Punchihewa, P. P. Infelta and M. Grätzel, *Langmuir*, 1991, **7**, 3012–3018.
29 E. Hao, N. A. Anderson, J. B. Asbury and T. Lian, *J. Phys. Chem. B*, 2002, **106**, 10191–10198.
30 L. G. C. Rego and V. S. Batista, *J. Am. Chem. Soc.*, 2003, **125**, 7989–7997.
31 S. G. Abuabara, L. G. C. Rego and V. S. Batista, *J. Am. Chem. Soc.*, 2005, **127**, 18234–18242.
32 E. Galoppini, *Coord. Chem. Rev.*, 2004, **248**, 1283–1297.
33 E. Bae, W. Choi, J. Park, H. S. Shin, S. B. Kim and J. S. Lee, *J. Phys. Chem. B*, 2004, **108**, 14093–14101.
34 K. S. Finnie, J. R. Bartlett and J. L. Woolfrey, *Langmuir*, 1998, **14**, 2744–2749.
35 K. Kilså, E. I. Mayo, B. S. Brunschwig, H. B. Gray, N. S. Lewis and J. R. Winkler, *J. Phys. Chem. B*, 2004, **108**, 15640–15651.
36 P. Falaras, *Sol. Energy Mater. Sol. Cells*, 1998, **53**, 163–175.
37 K. Hara, H. Sugihara, Y. Tachibana, A. Islam, M. Yanagida, K. Sayama and H. Arakawa, *Langmuir*, 2001, **17**, 5992–5999.
38 Y. Tachibana, J. E. Moser, M. Grätzel, D. R. Klug and J. R. Durrant, *J. Phys. Chem.*, 1996, **100**, 20056–20062.
39 K. Sayama, K. Hara, H. Sugihara, H. Arakawa, N. Mori, M. Satsuki, S. Suga, S. Tsukagoshi and Y. Abe, *Chem. Commun.*, 2000, 1173–1174.
40 K. Hara, K. Sayama, H. Arakawa, Y. Ohga, A. Shinpo and S. Suga, *Chem. Commun.*, 2001, 569–570.
41 C. Brückner, P. C. Foss, J. O. Sullivan, R. Pelto, M. Zeller, R. R. Birge and G. Crundwell, *Phys. Chem. Chem. Phys.*, 2006, **8**, 2402–2412.
42 F. Odobel, E. Blart, M. Lagrée, M. Villieras, H. Boujtita, N. El Murr, S. Caramori and C. Alberto Bignozzi, *J. Mater. Chem.*, 2003, **13**, 502–510.
43 K. Kilså, E. I. Mayo, D. Kuciauskas, R. Villahermosa, N. S. Lewis, J. R. Winkler and H. B. Gray, *J. Phys. Chem. A*, 2003, **107**, 3379–3383.
44 M. D. Newton, *Chem. Rev.*, 1991, **91**, 767–792.
45 K. D. Jordan and M. N. Paddon-Row, *Chem. Rev.*, 1992, **92**, 395–410.
46 N. A. Anderson, X. Ai, D. Chen, D. L. Mohler and T. Lian, *J. Phys. Chem. B*, 2003, **107**, 14231–14239.
47 H. P. E. Bae, J.-J. Lee, J. Park and W. Choi, *J. Phys. Chem. B*, 2006, **110**, 8740–8749.
48 E. Bae and W. Choi, *J. Phys. Chem. B*, 2006, **110**, 14792–14799.
49 P. Qu and G. J. Meyer, *Langmuir*, 2001, **17**, 6720–6728.
50 A. Merrins, C. Kleverlaan, G. Will, S. N. Rao, F. Scandola and D. Fitzmaurice, *J. Phys. Chem. B*, 2001, **105**, 2998–3004.
51 I. Gillaizeau-Gauthier, F. Odobel, M. Alebbi, R. Argazzi, E. Costa, C. A. Bignozzi, P. Qu and G. J. Meyer, *Inorg. Chem.*, 2001, **40**, 6073–6079.
52 W.-C. Liaw and K.-P. Chen, *Eur. Polym. J.*, 2007, **43**, 2265–2278.
53 N. Iguchi, C. Cady, R. C. Snoeberger III, B. M. Hunter, E. M. Sproviero, C. A. Schmuttenmaer, R. H. Crabtree, G. W. Brudvig and V. S. Batista, *Proc. SPIE–Int. Soc. Opt. Eng.*, 2008, **7034**, 70340C.
54 S. A. Haque, Y. Tachibana, R. L. Willis, J. E. Moser, M. Grätzel, D. R. Klug and J. R. Durrant, *J. Phys. Chem. B*, 2000, **104**, 538–547.
55 G. Ramakrishna, S. Verma, A. Jose, D. K. K. A. Das, D. K. Palit and H. N. Ghosh, *J. Phys. Chem. B*, 2006, **110**, 9012–9021.
56 B. I. Lemon and J. T. Hupp, *J. Phys. Chem. B*, 1999, **103**, 3797–3799.

57 I. Montanari, J. Nelson and J. R. Durrant, *J. Phys. Chem. B*, 2002, **106**, 12203–12210.

58 A. J. Nozik, *Phys. E.*, 2002, **14**, 115–120.

59 C. Lambert and G. Nöll, *Angew. Chem., Int. Ed.*, 1998, **37**, 2107–2110.

60 S. Pavasupree, S. Ngamsinlapasathian, M. Nakajima, Y. Suzuki and S. Yoshikawa, *J. Photochem. Photobiol., A*, 2006, **184**, 163–169.

61 A. B. F. Martinson, J. W. Elam, J. T. Hupp and M. J. Pellin, *Nano Lett.*, 2007, **7**, 2183–2187.

62 G. Wang, Q. Wang, W. Lu and J. Li, *J. Phys. Chem. B*, 2006, **110**, 22029–22034.

63 X. Feng, K. Shankar, O. K. Varghese, M. Paulose, T. J. Latempa and C. A. Grimes, *Nano Lett.*, 2008, **8**, 3781–3786.

64 K. Pan, Y. Dong, C. Tian, W. Zhou, G. Tian, B. Zhao and H. Fu, *Electrochim. Acta*, 2009, **54**, 7350–7356.

65 W. Zhou, X. Liu, J. Cui, D. Liu, J. Li, H. Jiang, J. Wang and H. Liu, *CrystEngComm*, 2011, **13**, 4557–4563.

66 J. Lin, J. Shen, R. Wang, J. Cui, W. Zhou, P. Hu, D. Liu, H. Liu, J. Wang, R. I. Boughton and Y. Yue, *J. Mater. Chem.*, 2011, **21**, 5106–5113.

67 K. S. Jeon, S. D. Oh, Y. D. Suh, H. Yoshikawa, H. Masuhara and M. Yoon, *Phys. Chem. Chem. Phys.*, 2009, **11**, 534–542.

68 Y. Qiu, W. Chen and S. Yang, *J. Mater. Chem.*, 2010, **20**, 1001–1006.

69 A. E. Suliman, Y. Tang and L. Xu, *Sol. Energy Mater. Sol. Cells*, 2007, **91**, 1658–1662.

70 H. Rensmo, K. Keis, H. Lindström, S. Södergren, A. Solbrand, A. Hagfeldt, L. N. Wang and M. Muhammed, *J. Phys. Chem. B*, 1997, **101**, 2598–2601.

71 Q. Zhang, C. S. Dandeneau, X. Zhou and G. Cao, *Adv. Mater.*, 2009, **21**, 4087–4108.

72 W. Zhou, H. Liu, R. I. Boughton, G. Du, J. Lin, J. Wang and D. Liua, *J. Mater. Chem.*, 2010, **20**, 5993–6008.

73 Q. Wei, K. Hirota, K. Tajima and K. Hashimoto, *Chem. Mater.*, 2006, **18**, 5080–5087.

74 E. Galoppini, J. Rochford, H. Chen, G. Saraf, Y. Lu, A. Hagfeldt and G. Boschloo, *J. Phys. Chem. B*, 2006, **110**, 16159–16161.

75 H. Gao, G. Fang, M. Wang, N. Liu, L. Yuan, C. Li, L. Ai, J. Zhang, C. Zhou, S. Wu and X. Zhao, *Mater. Res. Bull.*, 2008, **43**, 3345–3351.

76 J. Tornow and K. Schwarzburg, *J. Phys. Chem. C*, 2007, **111**, 8692–8698.

77 J. Jiu, S. Isoda, F. Wang and M. Adachi, *J. Phys. Chem. B*, 2006, **110**, 2087–2092.

78 B. H. Lee, M. Y. Song, S.-Y. Jang, S. M. Jo, S.-Y. Kwak and D. Y. Kim, *J. Phys. Chem. C*, 2009, **113**, 21453–22145.

79 Z. H. Chen, Y. B. Tang, C. P. Liu, Y. H. Leung, G. D. Yuan, L. M. Chen, Y. Q. Wang, I. Bello, J. A. Zapien, W. J. Zhang, C. S. Lee and S. T. Lee, *J. Phys. Chem. C*, 2009, **113**, 13433–13437.

80 P. Ravirajan, A. M. Peiró, M. K. Nazeeruddin, M. Graetzel, D. D. C. Bradley, J. R. Durrant and J. Nelson, *J. Phys. Chem. B*, 2006, **110**, 7635–7639.

81 K. Takanezawa, K. Hirota, Q.-S. Wei, K. Tajima and K. Hashimoto, *J. Phys. Chem. C*, 2007, **111**, 7218–7223.

82 Y.-Y. Lin, T.-H. Chu, S.-S. Li, C.-H. Chuang, C.-H. Chang, W.-F. Su, C.-P. Chang, M.-W. Chu and C.-W. Chen, *J. Am. Chem. Soc.*, 2009, **131**, 3644–3649.

83 L. Gai, G. Du, Z. Zuo, Y. Wang, D. Liu and H. Liu, *J. Phys. Chem. C*, 2009, **113**, 7610–7615.

84 I. C. Flores, J. N. d. Freitas, C. Longo, M.-A. D. Paoli, H. Winnischofer and A. F. Nogueira, *J. Photochem. Photobiol., A*, 2007, **189**, 153–160.

85 G. K. Mor, K. Shankar, M. Paulose, O. K. Varghese and C. A. Grimes, *Nano Lett.*, 2006, **6**, 215–218.

86 Z. Liu and M. Misra, *ACS Nano*, 2010, **4**, 2196–2200.

87 S. H. Ko, D. Lee, H. W. Kang, K. H. Nam, J. Y. Yeo, S. J. Hong, C. P. Grigoropoulos and H. J. Sung, *Nano Lett.*, 2011, **11**, 666–671.

88 E. Ghadiri, N. Taghavinia, S. M. Zakeeruddin, M. Grätzel and J. E. Moser, *Nano Lett.*, 2010, **10**, 1632–1638.